

Crystal structure, magnetic properties, and the magnetocaloric effect of Gd₅Rh₄ and GdRh

C. L. Wang, J. D. Zou, J. Liu, Y. Mudryk, K. A. Gschneidner Jr., Y. Long, V. Smetana, G. J. Miller, and V. K. Pecharsky

Citation: *Journal of Applied Physics* **113**, 17A904 (2013); doi: 10.1063/1.4793775

View online: <http://dx.doi.org/10.1063/1.4793775>

View Table of Contents: <http://scitation.aip.org/content/aip/journal/jap/113/17?ver=pdfcov>

Published by the AIP Publishing

Articles you may be interested in

[Study of magnetocaloric effect in GdRhIn compound](#)

AIP Conf. Proc. **1512**, 1090 (2013); 10.1063/1.4791425

[Magnetic and magnetocaloric properties of the new rare-earth-transition-metal intermetallic compound Gd₃Co₂₉Ge₄B₁₀](#)

J. Appl. Phys. **111**, 07E333 (2012); 10.1063/1.3677658

[Phase relationships, and structural, magnetic, and magnetocaloric properties in the Ce₅Si₄ – Ce₅Ge₄ system](#)

J. Appl. Phys. **107**, 013909 (2010); 10.1063/1.3276211

[Structural and magnetothermal properties of the Gd₅Sb_xGe_{4-x} system](#)

J. Appl. Phys. **99**, 08Q102 (2006); 10.1063/1.2150811

[Preparation, crystal structure, magnetic and magnetothermal properties of \(Gd_xR_{5-x}\)Si₄, where R=Pr and Tb, alloys](#)

J. Appl. Phys. **89**, 1738 (2001); 10.1063/1.1335821

A promotional banner for AIP Applied Physics Reviews. On the left is a small image of a book cover titled 'AIP Applied Physics Reviews' showing a diagram of a device. The main background is blue with a glowing light effect. The text 'NEW Special Topic Sections' is prominently displayed in white. Below this, it says 'NOW ONLINE' in yellow, followed by 'Lithium Niobate Properties and Applications: Reviews of Emerging Trends' in white. The AIP Applied Physics Reviews logo is in the bottom right corner.

NEW Special Topic Sections

NOW ONLINE
Lithium Niobate Properties and Applications:
Reviews of Emerging Trends

AIP Applied Physics
Reviews

Crystal structure, magnetic properties, and the magnetocaloric effect of Gd_5Rh_4 and GdRh

C. L. Wang,^{1,2,a)} J. D. Zou,¹ J. Liu,^{1,3} Y. Mudryk,¹ K. A. Gschneidner, Jr.,^{1,3} Y. Long,² V. Smetana,^{1,4} G. J. Miller,^{1,4} and V. K. Pecharsky^{1,3}

¹The Ames Laboratory, U.S. Department of Energy, Iowa State University, Ames, Iowa 50011-3020, USA

²School of Materials Science and Engineering, University of Science and Technology of Beijing, Beijing 100083, People's Republic of China

³Department of Materials Science and Engineering, Iowa State University, Ames, Iowa 50011-2300, USA

⁴Department of Chemistry, Iowa State University, Ames, Iowa 50011-3111, USA

(Presented 15 January 2013; received 30 October 2012; accepted 20 November 2012; published online 4 March 2013)

The crystal structures of Gd_5Rh_4 and GdRh have been studied by powder and single crystal x-ray diffraction. The results show that Gd_5Rh_4 is isotypic with Pu_5Rh_4 and the bond length of the short Rh-Rh dimer is 2.943(4) Å. According to heat capacity measurements in zero magnetic field, the magnetic ordering temperature of Gd_5Rh_4 is 13 K, in agreement with magnetization measurements. Both the heat capacity peak shape and the positive slope of the Arrott plots at Curie temperature (T_C) indicate the second-order nature of the magnetic transition. The temperature dependence of magnetization of Gd_5Rh_4 measured in 1 kOe applied field indicates noncollinear magnetic ordering that may change into nearly collinear ferromagnetic ordering by increasing the magnetic field. GdRh is ferromagnetic below $T_C = 22$ K. Moderate magnetocaloric effects and relatively high refrigerant capacities are observed in Gd_5Rh_4 and GdRh . © 2013 American Institute of Physics. [<http://dx.doi.org/10.1063/1.4793775>]

The compounds $\text{Gd}_5(\text{Si}_{1-x}\text{Ge}_x)_4$ have received considerable attention since the discovery of a giant magnetocaloric effect in $\text{Gd}_5\text{Si}_2\text{Ge}_2$.¹ Soon after, giant magnetostriction and giant magnetoresistance were also found in the $\text{Gd}_5(\text{Si}_{1-x}\text{Ge}_x)_4$ compounds.^{2,3} In this family of compounds, the magneto-responsive effects are intimately related to the peculiar crystal structure that is composed from two-dimensional slabs.⁴ The Si/Ge-Si/Ge interslab bonds, which can be broken and reformed by changing temperature, pressure, magnetic field, and chemical composition,^{2,4-6} have a strong influence on the magnetic properties of all $\text{Gd}_5(\text{Si}_{1-x}\text{Ge}_x)_4$ compounds.

So far, the Gd_5T_4 systems ($\text{T} = \text{Si}, \text{Ge}, \text{Sn}, \text{Pb}, \text{In}, \text{Ga}, \text{Sb}$) have been studied at various depths, especially the silicides and germanides.⁷ Rhodium, a transition metal, when combined with gadolinium, forms the compound Gd_5Rh_4 which has the Gd_5Si_4 -type structure (space group $Pnma$).⁸ However, the magnetic properties of Gd_5Rh_4 are, as yet, unreported. GdRh , which is found as a minor impurity in our Gd_5Rh_4 alloy, is a material with interesting properties, such as large specific heat and substantial ductility.⁹⁻¹¹ However, detailed magnetic data and magnetic entropy changes in varying magnetic fields has not been reported for GdRh . This work reports the crystal structures determined from both powder and single crystal diffraction data, magnetic properties, and magnetocaloric effects of Gd_5Rh_4 and GdRh .

Gd_5Rh_4 and GdRh were prepared by arc-melting the constituents in an argon atmosphere. Elemental Gd, with

purity exceeding 99.9 wt. % with respect to all elements in the Periodic Table, was prepared by the Materials Preparation Center¹² of the Ames Laboratory, and Rh metal, with purity of 99.99 wt. %, was purchased from a commercial vendor.

A Gd_5Rh_4 ingot was annealed in an evacuated silica tube at 1273 K for 7 days, and then quenched in an ice-water slurry. Phase analysis was performed by collecting the x-ray powder diffraction patterns, at room temperature on a PANalytical X'Pert Pro diffractometer using $\text{Cu K}\alpha_1$ radiation. A bulk GdRh sample was used for XRD due to its high ductility. The resulting XRD patterns were refined by the Rietveld methods using the LHPM RIETICA software.¹³ Magnetic properties were measured by using a superconducting quantum interference device (SQUID, MPMS-XL7) magnetometer from Quantum Design Inc. The zero-field heat capacity was measured in a physical properties measurement system (PPMS) from Quantum Design Inc.

A single crystal of $\text{Gd}_5\text{Rh}_4 \sim 0.10 \times 0.08 \times 0.06 \text{ mm}^3$ was extracted from the annealed sample and used for the crystal structure determination. It was mounted on a Bruker APEX CCD single crystal diffractometer equipped with graphite-monochromated $\text{Mo K}\alpha$ ($\lambda = 0.71069 \text{ Å}$) radiation. Room temperature intensity data were collected in an ω -scan mode over $2\theta = \sim 7^\circ - 57^\circ$ with exposure times of 10 s per frame. The reflections in the dataset were consistent with orthorhombic symmetry. Data integration, Lorentz polarization, and other corrections were completed by the SAINT subprogram included in the SMART software package.¹⁴ An empirical absorption correction was performed using the subprogram SADABS.¹⁵ The starting atomic parameters derived via direct methods and the program SIR 97 (Ref. 16) were

^{a)} Author to whom correspondence should be addressed. Electronic mail: chaolunwang@gmail.com. Current address: No. 30 Xueyuan Road, Haidian District, Beijing 100083, People's Republic of China.

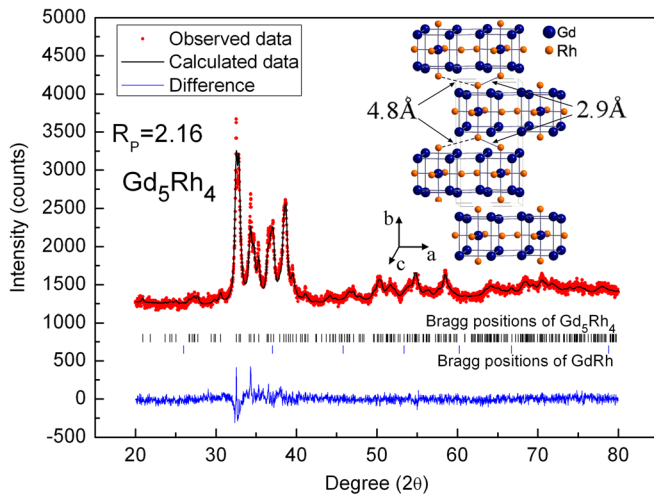


FIG. 1. XRD patterns and refinements of Gd_5Rh_4 . The inset shows the crystal structures of Gd_5Rh_4 .

subsequently refined using the program SHELX-97 (Ref. 17) (full-matrix least-squares on F^2) with anisotropic atomic displacement parameters calculated for all atoms.

The XRD pattern of Gd_5Rh_4 , shown in Fig. 1, corresponds to the Pu_5Rh_4 -type structure (space group $Pnma$). The weight percentage of the impurity phase GdRh is about 4% as determined by Rietveld refinement. Lattice parameters and unit cell volume of Gd_5Rh_4 derived from the Rietveld refinement of the powder XRD data are close to those reported previously⁸ and are listed in Table I. Atomic parameters of Gd_5Rh_4 at 293 K determined by the single crystal XRD data are listed in Table II. The final R values are: $R1 = 0.057$, $\omega R2 = 0.095$. The single crystal XRD data also confirm that Gd_5Rh_4 crystallizes in the Pu_5Rh_4 -type orthorhombic structure, and the length of the short and long Rh-Rh dimers are 2.943(4) and 4.847(4) Å, respectively. GdRh crystallizes in the cubic CsCl-type structure (space group $Pm\bar{3}m$), not shown here, and the lattice parameter is 3.447(1) Å, which is in agreement with the previously reported value of 3.440(2) Å.¹⁸

The zero-field-cooled-heating (ZFC) and field-cooled-cooling (FCC) magnetization curves of Gd_5Rh_4 measured in different magnetic fields are shown in Fig. 2. The cusp observed in ZFC and FCC curves in 1 kOe magnetic field at 14 K indicates the existence of weak antiferromagnetic interactions at low temperature. However, when the magnetic field is larger than 10 kOe, the ZFC and FCC curves exhibit a ferromagnetic-like ordering. The fully reversible ZFC and FCC curves at the transition temperature indicate a second-order transition, which is consistent with the “ λ ” type anomaly of the heat capacity data (not shown here) at 13 K in zero magnetic field and the positive slope of the Arrott plot shown in Fig. 3(c). The paramagnetic Curie temperature and effective magnetic moment calculated from the inverse

TABLE I. Lattice parameters of Gd_5Rh_4 obtained from the powder XRD pattern at room temperature (space group $Pnma$).

a (Å)	b (Å)	c (Å)	Volume	References
7.342(1)	14.539(3)	7.521(1)	802.8(3)	This study
7.343	14.57	7.527	805.2	Ref. 8

TABLE II. Atomic parameters of Gd_5Rh_4 determined by single crystal x-ray diffraction at 293 K.

Atom	Site	Occupancy	x	y	z	U_{eq} (Å ²)
Gd1	8d	1	0.1612(2)	0.6226(1)	0.1660(2)	0.0146(2)
Gd2	4c	1	0.1806(2)	1/4	0.0125(2)	0.0158(3)
Gd3	8d	1	0.4964(2)	0.0914(1)	0.1795(1)	0.0158(2)
Rh1	8d	1	0.3189(3)	0.5398(1)	0.4661(2)	0.0181(4)
Rh2	4c	1	0.3102(4)	1/4	0.3527(4)	0.0219(6)
Rh3	4c	1	0.0441(4)	1/4	0.6011(4)	0.0216(6)

susceptibility fitting of the 10 kOe ZFC magnetization curve from 100 K to 250 K (not shown here) are, respectively, 24 K and $7.84 \mu_B/\text{Gd}$ atom (close to the theoretical value of $7.94 \mu_B$ for the free Gd^{3+} ion). The positive paramagnetic Curie temperature of Gd_5Rh_4 indicates dominant ferromagnetic interactions, which is similar with the Gd_5T_4 ($\text{T} = \text{Si}, \text{Ge}$) compounds. The magnetization of Gd_5Rh_4 is far from saturation in 50 kOe field, as shown in Fig. 3(a), indicating that even in 50 kOe the ferromagnetic order is not fully collinear.

The inset of Fig. 2 shows a magnetic transition of GdRh from a ferromagnetic to paramagnetic state at 22 K in 100 Oe magnetic field. The absence of hysteresis in the magnetization curves at the Curie temperature indicates a second-order transition, which agrees with the earlier report of the “ λ ” type anomaly in the heat capacity⁹ and the positive slope of the Arrott plot shown in Fig. 3(d).

The entropy change $\Delta S(T, H)$ of Gd_5Rh_4 and GdRh have been calculated from the isothermal magnetization curves using the Maxwell relation $\Delta S(T, H) = \int_0^H (\partial M / \partial T)_H dH$. The maximum entropy changes of Gd_5Rh_4 and GdRh , shown in Fig. 4, are 14 J/kg·K (at 16 K and 50 kOe) and 22 J/kg·K (at 24 K and 50 kOe), respectively. The relative cooling power (RCP) was estimated using the following equation $RCP = -\Delta S^{\max} \times \delta T_{FWHM}$, where δT_{FWHM} is the full width at half maximum of $|\Delta S|$ vs. T curve. The RCPs of Gd_5Rh_4 and GdRh for a magnetic field change of 0-50 kOe are 374 J/kg and 534 J/kg, respectively.

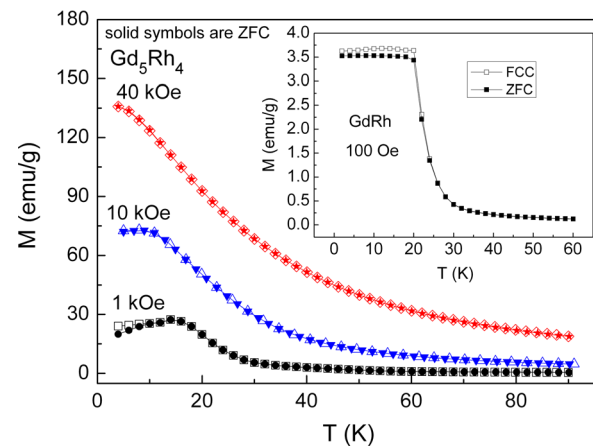


FIG. 2. The temperature dependence of magnetization of Gd_5Rh_4 in 1, 10, and 40 kOe magnetic fields from 4 to 90 K. The solid and hollow symbols represent the ZFC and FCC data, respectively. The inset shows ZFC and FCC curves of GdRh in a 100 Oe magnetic field.

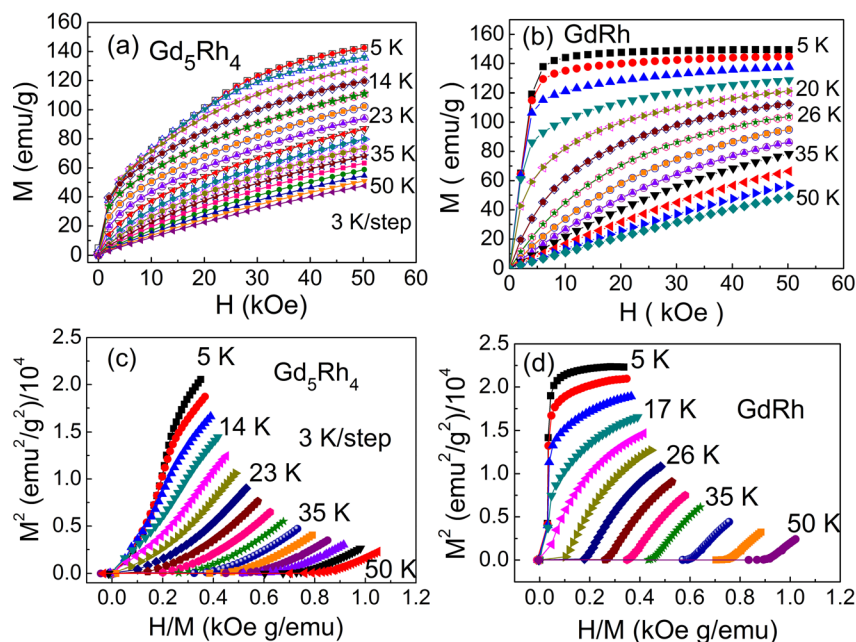


FIG. 3. Isothermal magnetization curves of Gd_5Rh_4 (a) and $GdRh$ (b) from 5 K to 50 K, and Arrott plots of Gd_5Rh_4 (c) and $GdRh$ (d).

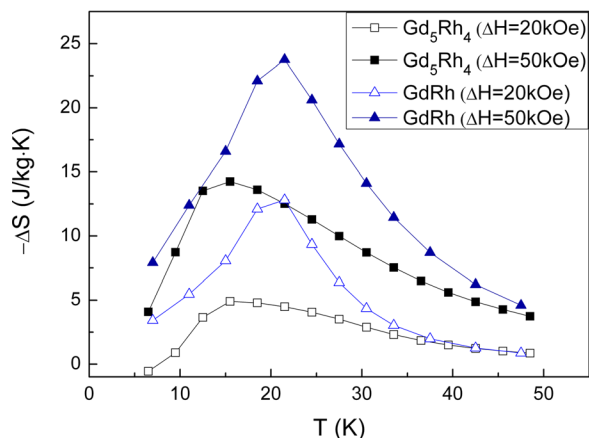


FIG. 4. The magnetic entropy changes of Gd_5Rh_4 and $GdRh$ obtained for 0–20 and 0–50 kOe field changes.

The crystal structures of Gd_5Rh_4 (Pu_5Rh_4 -type) and $GdRh$ (CsCl-type) have been confirmed by means of x-ray single crystal and powder diffraction. The $M(T)$ curves of Gd_5Rh_4 indicate the existence of a weak antiferromagnetic interaction in the ground state which can be changed to a predominantly ferromagnetic interactions by increasing magnetic field, although the magnetization curve does not saturate at 5 K in a 50 kOe field. The magnetic transitions in Gd_5Rh_4 and $GdRh$ at 13 K and 22 K, respectively, have second-order character. Both Gd_5Rh_4 and $GdRh$ have moderate magnetocaloric effects (MCEs) of $\Delta S^{\max} = 14$ J/kg·K and 22 J/kg·K for $\Delta H = 50$ kOe, respectively. The former is significantly smaller than that of $ErAl_2$ (37 J/kg·K, $T_C = 13.6$ K), which may be due to the antiferromagnetic interaction in Gd_5Rh_4 . The $GdRh$ value, however, is comparable with that of $DyNi_2$ (21 J/kg·K, $T_C = 20.5$ K).¹⁹

The Ames Laboratory is operated for the U.S. Department of Energy by Iowa State University of Science and Technology. This work was supported by the Department of

Energy, Office of Basic Energy Sciences, Materials Sciences Division under Contract No. DE-AC02-07CH11358. C.L.W. and Y.L. acknowledge the National Science Foundation of China, the National High Technology Research and Development Program of China, the National Basic Research Program of China, and the funding from China Scholarship Council for support of C.L.W. stay at the Ames Laboratory.

- ¹V. K. Pecharsky and K. A. Gschneidner, Jr., *Phys. Rev. Lett.* **78**, 4494 (1997).
- ²L. Morellon, P. A. Algarabel, M. R. Ibarra, J. Blasco, B. Garcia-Landa, Z. Arnold, and F. Albertini, *Phys. Rev. B* **58**, R14721 (1998).
- ³L. Morellon, J. Stankiewicz, B. Garcia-Landa, P. A. Algarabel, and M. R. Ibarra, *Appl. Phys. Lett.* **73**, 3462 (1998).
- ⁴W. Choe, V. K. Pecharsky, A. O. Pecharsky, K. A. Gschneidner, V. G. Young, and G. J. Miller, *Phys. Rev. Lett.* **84**, 4617 (2000).
- ⁵L. Morellon, J. Blasco, P. A. Algarabel, and M. R. Ibarra, *Phys. Rev. B* **62**, 1022 (2000).
- ⁶V. Pecharsky and K. A. Gschneidner, Jr., *J. Alloys Compd.* **260**, 98 (1997).
- ⁷V. K. Pecharsky and K. A. Gschneidner, *Pure Appl. Chem.* **79**, 1383 (2007).
- ⁸A. Raman, *J. Less-Common Met.* **48**, 111 (1976).
- ⁹A. A. Azhar, C. D. Mitescu, W. R. Johanson, C. B. Zimm, and J. A. Barclay, *J. Appl. Phys.* **57**, 3235 (1985).
- ¹⁰K. H. J. Buschow, J. F. Olijhoek, and A. R. Miedema, *Cryogenics* **15**, 261 (1975).
- ¹¹K. A. Gschneidner, A. O. Pecharsky, and V. K. Pecharsky, in *Cryocoolers 13*, edited by R. G. Ross (Springer, US, 2005), p. 363.
- ¹²See www.mpc.ameslab.gov for Materials Preparation Center, The Ames Laboratory of U.S. Department of Energy, Ames, IA, USA.
- ¹³B. A. Hunter, Rietica—A Visual Rietveld Program, International Union of Crystallography Commission on Powder Diffraction Newsletter No. 20, Summer, 1998, see <http://www.rietica.org>.
- ¹⁴SMART ed., Bruker Analytical X-ray Systems, Inc., Madison, WI, 2000.
- ¹⁵R. H. Blessing, *Acta Crystallogr. A* **51**, 33 (1995).
- ¹⁶A. Altomare, M. Burla, M. Camalli, B. Carroccini, G. Cascarano, C. Giacovazzo, A. Guagliardi, A. Moliterni, G. Polidori, and R. Rizzi, *J. Appl. Crystallogr.* **32**, 115 (1999).
- ¹⁷G. M. Sheldrick, *SHELXL-97: Program for the Refinement of Crystal Structures* (University of Göttingen, Germany, 1997).
- ¹⁸A. E. Dwight, R. A. Conner, Jr., and J. W. Downey, *Acta Crystallogr.* **18**, 835 (1965).
- ¹⁹P. J. von Ranke, V. K. Pecharsky, and K. A. Gschneidner, Jr., *Phys. Rev. B* **58**, 12110 (1998).